Impact of phytoplankton on the biogeochemical cycling of iron in subantarctic waters southeast of New Zealand during FeCycle

R. M. L. McKay,[1] S. W. Wilhelm,[2] J. Hall,[3] D. A. Hutchins,[4] M. M. D. Al-Rshaidat,[1] C. E. Mioni,[2] S. Pickmere,[3] D. Porta,[1] and P. W. Boyd[5]

Received 13 February 2005; revised 20 October 2005; accepted 26 October 2005; published 21 December 2005.

[1] During austral summer 2003, we tracked a patch of surface water infused with the tracer sulfur hexafluoride, but without addition of Fe, through subantarctic waters over 10 days in order to characterize and quantify algal Fe pools and fluxes to construct a detailed biogeochemical budget. Nutrient profiles characterized this patch as a high-nitrate, low-silicic acid, low-chlorophyll (HNLSiLC) water mass deficient in dissolved Fe. The low Fe condition was confirmed by several approaches: shipboard iron enrichment experiments and physiological indices of Fe deficiency ($F_v/F_m < 0.25$, Ferredoxin Index < 0.2). During FeCycle, picophytoplankton (0.2–2 μm) and nanophytoplankton (2–20 μm) each contributed >40% of total chlorophyll. Whereas the picophytoplankton accounted for ~50% of total primary production, they were responsible for the majority of community iron uptake in the mixed layer. Thus ratios of ^{55}Fe:^{14}C uptake were highest for picophytoplankton (median: 17 μmol:mol) and declined to ~5 μmol:mol for the larger algal size fractions. A pelagic Fe budget revealed that picophytoplankton were the largest pool of algal Fe (>90%), which was consistent with the high (~80%) phytoplankton Fe demand attributed to them. However, Fe regenerated by herbivory satisfied only ~20% of total algal Fe demand. This iron regeneration term increased to 40% of algal Fe demand when we include Fe recycled by bacterivory. As recycled, rather than new, iron dominated the pelagic iron budget (Boyd et al., 2005), it is highly unlikely that the supply of new Fe would redress the imbalance between algal Fe demand and supply. Reasons for this imbalance may include the overestimation of algal iron uptake from radiotracer techniques, or a lack of consideration of other iron regeneration processes. In conclusion, it seems that algal Fe uptake cannot be supported solely by the recycling of algal iron, and may require an Fe "subsidy" from that regenerated by heterotrophic pathways.

Citation: McKay, R. M. L., S. W. Wilhelm, J. Hall, D. A. Hutchins, M. M. D. Al-Rshaidat, C. E. Mioni, S. Pickmere, D. Porta, and P. W. Boyd (2005), Impact of phytoplankton on the biogeochemical cycling of iron in subantarctic waters southeast of New Zealand during FeCycle, *Global Biogeochem. Cycles*, *19*, GB4S24, doi:10.1029/2005GB002482.

1. Introduction

[2] Mesoscale in situ fertilization experiments have demonstrated that low availability of Fe controls phytoplankton growth, community structure and ecosystem function in high-nitrate, low-chlorophyll (HNLC) oceanic provinces that include the equatorial Pacific [*Coale et al.*, 1996], the subarctic Pacific [*Tsuda et al.*, 2003; *Boyd et al.*, 2004a] and the Southern Ocean [*Boyd et al.*, 2000]. In these regions, major nutrients are present in excess and the addition of Fe promotes phytoplankton blooms, resulting in a switch in the ecosystem from recycling- to export-dominated planktonic communities [*Boyd et al.*, 2004a].

[3] Given the importance of Fe as a global regulator of production, there have been numerous attempts to model the oceanic Fe cycle on both regional [*Price and Morel*, 1998; *Tortell et al.*, 1999; *Bowie et al.*, 2001] and global scales [e.g., *Fung et al.*, 2000; *Parekh et al.*, 2004]. Among the key parameters in these models is the partitioning of Fe within suspended particles (i.e., scavenged versus interior pools), and Fe quotas of the pelagic biota. Yet actual measurements of these parameters in marine ecosystems are not widely available, and modelers investigating the biogeochemical

[1]Department of Biological Sciences, Bowling Green State University, Bowling Green, Ohio, USA.
[2]Center for Environmental Biotechnology and Department of Microbiology, University of Tennessee, Knoxville, Tennessee, USA.
[3]National Institute of Water and Atmospheric Research, Hamilton, New Zealand.
[4]Graduate College of Marine Studies, University of Delaware, Lewes, Delaware, USA.
[5]National Institute of Water and Atmospheric Research, Centre for Chemical and Physical Oceanography, Department of Chemistry, University of Otago, Dunedin, New Zealand.

0886-6236/05/2005GB002482$12.00

cycle of Fe have been forced to rely mainly on values obtained from laboratory studies using model algal species.

[4] The general intent of FeCycle was to improve on previous pelagic Fe budgets for HNLC waters [*Landry et al.*, 1997; *Price and Morel*, 1998; *Bowie et al.*, 2001] by better determining the magnitude of the pools of Fe, the fluxes between them, and the timescales on which they turn over. FeCycle tracked a sulfur hexafluoride (SF_6) labeled patch of surface water in high-nitrate, low-silicic acid, low-chlorophyll (HNLSiLC) subantarctic (SA) waters southeast of New Zealand for 10 days. The specific aim of this study was to determine the role and impact of phytoplankton on the biogeochemical cycling of iron in the upper ocean.

[5] The location chosen for FeCycle has been the focus of seasonal studies investigating both algal [*Chang and Gall*, 1998] and microbial [*Hall et al.*, 1999] community structure, ecosystem tropho-dynamics [*Bradford-Grieve et al.*, 1999] and the effects of Fe perturbation on these properties [*Boyd et al.*, 1999]. Furthermore, this region has been monitored via a coupled bio-optical and deep sediment trap mooring deployed since October 2001 [*Nodder et al.*, 2005].

[6] The circumpolar SA water mass, located between the Subtropical Convergence and the Polar Front, covers approximately one tenth of world ocean surface area [*Banse and English*, 1997], yet has received little attention compared to waters south of the Polar Front. In particular, knowledge of environmental factors that constrain production in SA HNLC waters have only begun to be understood [*Boyd*, 2002]. From the few studies that have addressed this issue, there emerges a seasonal pattern of factors that control primary production in SA waters with light limitation being a potentially controlling variable in winter, and low availability of Fe and both Fe and silicic acid in spring and summer, respectively [*Boyd et al.*, 1999; *Sedwick et al.*, 1999; *Hutchins et al.*, 2001]. A close coupling between iron-limited algal growth and efficient grazing by microzooplankton is likely responsible for maintaining perennially low algal stocks in HNLC regions [*Strom et al.*, 2000], including SA waters [*Banse*, 1996; *Hall et al.*, 2004].

[7] The FeCycle experiment attempted to develop a pelagic Fe budget in a water mass where primary production is reported as constrained by low Fe availability. Although low levels of silicic acid exert additional controls on the endemic diatom community [*Hutchins et al.*, 2001; *Leblanc et al.*, 2005], silicic acid deficiency was not expected to impact the rates of primary production by picophytoplankton that dominate the endemic phytoplankton assemblage in SA waters [*Bradford-Grieve et al.*, 1997, 1999; *Hutchins et al.*, 2001]. Moreover, light was not anticipated to impose substantial controls on primary production since mixed layer depth is relatively shallow during austral summer [*Boyd et al.*, 1999; *Sedwick et al.*, 1999; *Hutchins et al.*, 2001], the period during which this study was conducted.

2. Study Site and Methods

2.1. Study Site and Tracer Release

[8] A survey conducted prior to FeCycle identified a candidate HNLSiLC site at 178.72°E, 46.24°S for the mesoscale tracer study [*Boyd et al.*, 2005]. The suitability of this location was assessed during an oceanographic survey comprising underway sampling for temperature, salinity, chlorophyll (chl), F_v/F_m, and dissolved nutrients [*Boyd et al.*, 2005]. Dissolved iron (Fe_d) was measured in underway samples collected using a clean tow-fish and pump system [*Boyd et al.*, 2005].

[9] SF_6 was released to the surface mixed layer at a depth of 7 m commencing at 0200 hours (local time) on 2 February 2003. No Fe was added along with the SF_6. After 12 hours, coverage of SF_6 had extended to an area of $\sim$49 km^2 [*Boyd et al.*, 2005]. Immediately following the tracer release, and each night thereafter, the areal extent of the SF_6-labeled patch was mapped during an underway survey of the patch.

2.2. Sampling

[10] Day 1 of FeCycle was nominally defined as 3 February 2003, and the final day of the experiment was 12 February (day 10). We conducted measurements at the patch centre, defined as the highest SF_6 concentration. Measurements were coordinated to provide upper ocean Fe budgets on 4 days (4, 5, 6 and 9 February). Sampling took place around local dawn at 15 m depth within the 40–45 m deep seasonal mixed layer. Water was always sampled using a metal–clean pump system.

2.3. Primary Production and Community Iron Uptake

[11] Size-fractionated chl *a* was determined from filtration of seston on polycarbonate membranes of 0.22, 2, 5 and 20 μm porosity based on the size classification scheme of *Sieburth et al.* [1978]. Chl was measured by fluorometry after *Welschmeyer* [1994]. Photochemical energy conversion efficiency was measured as F_v/F_m on dark-acclimated (0.5 hours), unfiltered samples using a FAST^{tracka} fast repetition rate fluorometer (FRRF; Chelsea Technologies Group).

[12] Algal carbon fixation and community Fe uptake were measured on samples incubated in wide mesh bags deployed in situ for $\sim$24 hours at depths of 3, 5, 8, 12, 20, 30 and 45 m under a doughnut-shaped surface float used to minimize shading of bottles at the shallowest depths. Carbon fixation based on radioisotope measurements and 24-hour incubations are reported to approximate net primary production [*Laws*, 1991]. Samples collected from 20 m depth into 300-mL acid-rinsed polycarbonate bottles were inoculated with 20 μCi of $NaH^{14}CO_3$ or $^{55}FeCl_3$ (added as Fe:EDTA; final concentration: 0.2 nmol kg^{-1} ^{55}Fe: 10 μM EDTA) for primary production and Fe uptake, respectively. This addition of Fe was chosen to mimic the inorganic Fe concentrations in situ whereas EDTA was included to minimize Fe hydrolysis and precipitation. Our choice of EDTA as a chelating agent has been validated by the results of *Maldonado et al.* [2005] who showed that community uptake of Fe complexed to EDTA proceeded at a rate comparable to that of Fe bound to in situ ligands.

[13] Upon recovery of the bottles, samples were filtered in series through 0.22-, 2-, 5- and 20-μm polycarbonate filters

using a size-fractionation tower [*Boyd and Harrison*, 1999]. Samples incubated with ^{14}C were rinsed with filtered seawater, followed by acidification to volatilize any remaining inorganic carbon [*Boyd and Harrison*, 1999]. Samples incubated with ^{55}Fe were rinsed with a reducing oxalate reagent to remove surface adsorbed Fe [*Tovar-Sanchez et al.*, 2003]. Filters were stored in a dessicator prior to scintillation counting.

[14] Short-term community Fe uptake was measured on samples inoculated with ^{55}Fe (added as Fe:EDTA; final concentration: 2.0 nmol kg^{-1} ^{55}Fe: 10 μM EDTA) and incubated for 6 hours in a flow-through (ambient seawater ±1°C) deckboard incubator with neutral density screening to reduce the light level to ~30% of incident. Following incubation, samples were filtered onto 0.22-μm polycarbonate membranes and rinsed with the oxalate reagent as described above prior to scintillation counting.

[15] Photosynthesis versus irradiance (PE) curves were generated by incubating samples inoculated with 10 μCi of $H^{14}CO_3$ simultaneously under 10 irradiances (5–500 μmol quanta m^{-2} s^{-1}) for 4 hours in a temperature-controlled photosynthetron. Following incubation, samples were filtered onto 0.22-μm polycarbonate membranes and acid-stable ^{14}C assimilation was measured by liquid scintillation counting. For each PE curve, the rates of photosynthesis were determined by using a nonlinear regression curve fitting function and the equation

$$P^{chl} = P_m^{chl}\left(1 - e\left[-\alpha^{chl} I / P_m^{chl}\right]\right),$$

where P^{chl} is the chl *a* normalized rate of photosynthesis at irradiance I, P_m^{chl} is the maximum rate of photosynthesis in the absence of photoinhibition, and α^{chl} is the initial slope of the PE curve.

2.4. Picophytoplankton and Nanoflagellate Biomass

[16] The abundance of the picophytoplankton (0.22–2 μm) was determined on unpreserved samples by flow cytometry using a FACSCalibur instrument (BD Biosciences) with CellQuest software [*Hall et al.*, 2004]. Double distilled water was used as sheath fluid and the analyzed volume was calculated using Trucount (BD Biosciences) beads as a tracer. Samples were run at Hi flow setting (~60 μL min^{-1}) with a minimum of 1.5×10^3 counts per sample. Determination of cell carbon was made assuming 250 fg C $cell^{-1}$ for cyanobacteria [*Li et al.*, 1992] and 920 fg C $cell^{-1}$ for eukaryotes [*Booth*, 1988].

[17] Duplicate samples collected for nanoflagellate enumeration were size-fractionated through a 20-μm nylon mesh. The filtrate was fixed with an equal volume of ice cold glutaraldehyde (2% final [v/v]) for 1 hour. Fixed samples were filtered onto 0.8-μm black Nucleopore filters, stained with primulin, mounted on slides and stored frozen. Nanoflagellates were enumerated using epifluorescence microscopy after *Hall et al.* [2004]. Nanophytoflagellates were differentiated using chl *a* under blue light excitation [*Hall et al.*, 2004]. Biovolumes were calculated from measurements on a minimum of 200 cells using dimensions and approximated geometric shape [*Chang*, 1988]. Cell carbon for autotrophic and heterotrophic nanoflagellate biomass was assumed to be 240 fg C μm^{-3} as reported by *Verity et al.* [1992].

2.5. Microphytoplankton Biomass

[18] Microphytoplankton were concentrated from the pumped seawater supply using a 20-μm mesh size net, followed by fractionation using 210-μm polypropylene mesh to remove mesozooplankton. Aliquots of the 20–210 μm fraction were either preserved in 2% [v/v] glutaraldehyde for microscopic analysis, used to measure F_v/F_m or used to determine the Ferredoxin (Fd) Index by Western immunoblotting after *Xia et al.* [2004]. Polyclonal antiserum raised against *Phaeodactylum tricornutum* flavodoxin (Flvd) [*La Roche et al.*, 1995] and *Thalassiosira weissflogii* Fd [*McKay et al.*, 1999] were used to probe replicate blots (n = 2–3). Immunoreactive proteins were visualized by chemifluorescence using the ECF substrate (Amersham Biosciences) followed by detection using a Storm 860 imaging system and analyzed using ImageQuant software (version 5.2; Amersham Biosciences).

[19] Microphytoplankton preserved in glutaraldehyde were identified using taxonomic keys [*Horner*, 2002] and enumerated by light microscopy using a Palmer-Maloney chamber. Iron quotas were determined for microphytoplankton samples collected on 11 February. In a trace metal clean lab, microphytoplankton were concentrated from pumped water using an acid-rinsed nylon plankton net. Splits of the sample were analyzed for F_v/F_m, floristics, Fd Index, particulate organic carbon, particulate organic nitrogen and for trace metals. For the latter, samples were processed to remove externally bound Fe using the oxalate reagent [*Tovar-Sanchez et al.*, 2003] prior to analysis as described by (R. D. Frew et al., Sinking particulate iron dynamics during FeCycle in subantarctic waters southeast of New Zealand, submitted to *Global Biogeochemical Cycles*, 2005) (hereinafter referred to as Frew et al., submitted manuscript, 2005).

2.6. Constructing a Phytoplankton Iron Budget

[20] During FeCycle, a budget was constructed using mean values for algal biomass, rates of algal Fe uptake and Fe:C molar ratios obtained over the four budget sampling days. Estimates of algal biomass were restricted to the picoplankton and the nanoflagellates. Because heterotrophic bacteria were unavoidably included in the picoplankton fraction during all incubation experiments, we account for their contribution to biogenic Fe in this size fraction using a conversion factor of 12.4 fg C $cell^{-1}$ [*Fukuda et al.*, 1998]. Net cellular Fe:C assimilation ratios were calculated as the mean of ^{55}Fe and ^{14}C uptake ratios at 12 m and 20 m depth for each size fraction over the four budget events. Specific caveats regarding the use of uptake rates to derive Fe:C ratios are addressed by *Strzepek et al.* [2005]. Ratios derived for the 2–5 μm and 5–20 μm nanophytoflagellates were combined to provide a mean Fe:C ratio to be applied to nanoflagellate biomass. We derived estimates of intracellular Fe associated with each size fraction as the product of biomass and cellular Fe:C. The contribution of lithogenic Fe to particulate Fe was estimated using crustal Al:Fe ratios (Frew et al., submitted manuscript, 2005). Phytoplankton Fe demand was calcu-

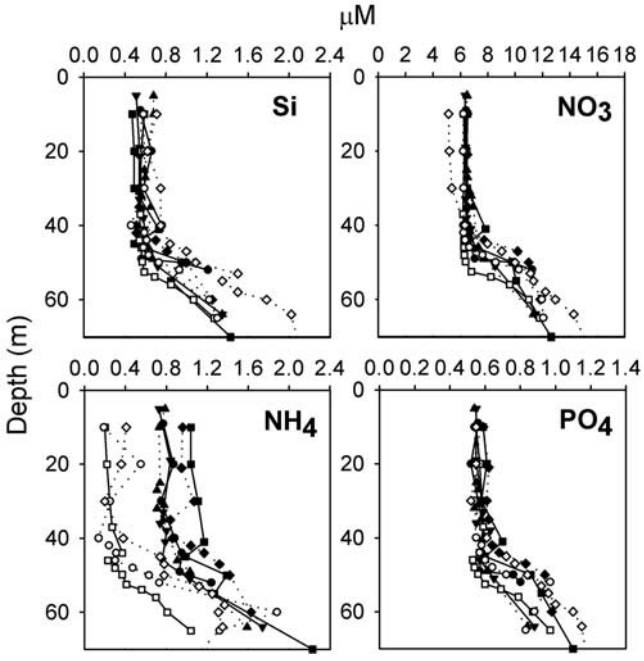

Figure 1. Upper ocean vertical profiles of dissolved macronutrients (Si, NO_3^-, NH_4^+, PO_4^-) corresponding to budget events 1–3 (3–6 February) and two diel sampling events (7 and 11 February): triangle pointing up, 3 February (1530 local time (LT)); triangle pointing down, 4 February (0245 LT); solid circle, 4 February (1410 LT); solid square, 5 February (0330 LT); solid diamond, 5 February (1150 LT); open square, 6 February (1130 LT); open circle, 7 February (1130 LT); open diamond, 11 February (2350 LT).

lated from mean ^{55}Fe uptake measured at 12 m and 20 m depth. For individual components of the picoplankton (cyanobacteria, eukaryotes and heterotrophic bacteria), we also included rates of steady state Fe demand reported in *Strzepek et al.* [2005]. Fe regeneration rates used in the budget were based on measured rates using ^{55}Fe-labeled picoplankton [*Strzepek et al.*, 2005].

2.7. Iron Perturbation Experiment

[21] We tested whether Fe availability was growth limiting to phytoplankton during FeCycle using a deckboard perturbation experiment. Water was collected from 10 m depth using the metal-clean sampling pump at 1800 hours on 3 and 6 February and desferrioxamine B (DFB; Sigma Chemical Co.) was added to withhold Fe from the community as described by *Eldridge et al.* [2004]. DFB was added to triplicate sets of acid-rinsed polycarbonate bottles to generate a series of DFB concentrations ranging from 1 to 10 nM. In parallel, triplicate sets of bottles were amended with $FeCl_3$ (dissolved in 0.01 M Ultrex HCl) to final concentrations ranging from 0.5 to 3 nmol kg^{-1} Fe in excess of ambient. Neither DFB nor Fe was added to control bottles. Sealed bottles were placed in a flow-through deckboard incubator lined with spectrum-correcting blue Plexiglas to simulate the light intensity and spectral quality of the 50% incident depth in the water column. Samples were collected only at the end point of the 72-hour experiment to reduce the potential for contamination during subsampling. Samples were analyzed for F_v/F_m and for determination of size-fractionated chl *a*. Cells were enumerated, and taxonomic affinity resolved, by flow cytometry. Dissolved nutrients were determined by shipboard automated analysis.

2.8. Statistical Analysis

[22] Data were subject to one-way analysis of variance (ANOVA) for independent samples followed by a Tukey Honestly Significance Difference (HSD) test using VassarStats: Web Site for Statistical Computation (http://faculty.vassar.edu/lowry/VassarStats.html). Specific analyses associated with the Fe perturbation experiments are described elsewhere [*Mioni et al.*, 2005].

3. Results and Discussion

3.1. Nutrient Profiles

[23] Dissolved macronutrients showed vertical upper ocean distribution profiles typical for HNLSiLC SA waters during austral summer [*Hutchins et al.*, 2001] (Figure 1) with nitrate concentrations of ~6 μM and silicic acid at submicromolar levels. The HNLSiLC condition is common throughout SA surface waters and is most evident during austral summer and autumn, when both silicic acid and Fe are typically depleted [*Boyd et al.*, 1999; *Sedwick et al.*, 1999; *Hutchins et al.*, 2001]. In summer, it has been suggested that diatom stocks are maintained at low levels due to a silicic acid-Fe colimitation [*Hutchins et al.*, 2001], a feature that was supported by results from FeCycle [*Leblanc et al.*, 2005].

[24] Two different methods were used to measure Fe_d during FeCycle. Flow injection analysis using chemiluminescence of Fe(II) demonstrated mixed layer Fe_d to be variable, ranging between 0.25 and 0.45 nmol kg^{-1} with the highest values evident as surface enrichment coinciding with budget event 4 of FeCycle (P. L. Croot, unpublished data, 2005). By contrast, Fe_d measured on acidified samples by graphite furnace atomic adsorption analysis varied little throughout FeCycle with values of ~0.07 nmol kg^{-1} (M. J. Ellwood, unpublished data, 2005).

[25] In general, macronutrient profiles were characterized by surface depletion through the mixed layer with a nutricline evident below 50 m depth (Figure 1). With the exception of ammonium, nutrient profiles were consistent throughout FeCycle. Nutricline depths for macronutrients were shallower and more coincident with the pycnocline compared with those of the Fe_d profiles (P. L. Croot, unpublished data, 2005) implying that the vertical diffusive resupply of nitrate and silicic acid from depth were greater than that of Fe_d [*Boyd et al.*, 2005].

3.2. Algal Stocks, Community Size Structure, and Composition

[26] The picophytoplankton, comprising both cyanobacteria and eukaryotes, accounted for between 33 and 46% (average = 41 ± 6%) of total chl *a* (Figure 2a) and numerically dominated the phytoplankton throughout FeCycle (Figure 2b). Picocyanobacteria ranged between 1 and 2 × 10^{11} cells m^{-3} and were tenfold more abundant

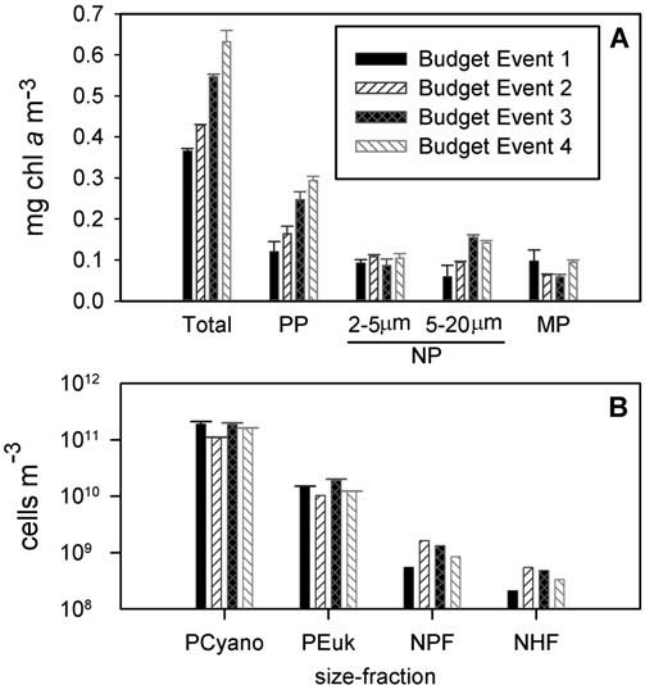

Figure 2. (a) Total and size-fractionated chl *a* and (b) cell abundance reported from budget event sampling (4, 5, 6, and 9 February). Figure 2a notations are: PP, picophytoplankton (0.2–2 μm); NP, nanophytoplankton; MP, microphytoplankton (>20 μm). Figure 2b notations are: PCyano, picocyanobacteria; PEuk, picoeukaryotes; NPF, nanophytoflagellates, NHF, nanoheteroflagellates.

than the picoeukaryotes and nearly 2 orders of magnitude more abundant than nanoflagellates (Figure 2b).

[27] Picoplankton are an important component of the phytoplankton of oligotrophic waters [*Stockner*, 1988] where primary production is supported mainly by nutrients regenerated via the microbial loop. Picoplankton are also the dominant phytoplankton assemblage in HNLC regions [e.g., *Cavendar-Bares et al.*, 1999] and are important contributors to both autotrophic biomass and primary production in SA waters [*Bradford-Grieve et al.*, 1999; *Hutchins et al.*, 2001].

[28] Collectively, the nanophytoplankton contributed comparable chl biomass (average: 43 ± 4%) to that of the picoplankton (Figure 2a). Autotrophs were dominant among nanoflagellates, both numerically, ranging from 0.5 to 2 × 10^9 cells m^{-3} (Figure 2b), and in terms of biomass, contributing >75% to total nanoflagellate carbon biomass. Although we did not resolve specific nanophytoplankton taxa, a companion study reported that dinoflagellates and the diatom *Cylindrotheca closterium* were the dominant taxa enumerated within this size class during budget event 1 [*Leblanc et al.*, 2005].

[29] *Chang and Gall* [1998] previously identified the nanoflagellates as an important assemblage in SA waters east of New Zealand. In their study, in which contributions from the picoplankton were not considered, the nanoflagellates contributed on average, 35% and 53% of cell carbon biomass during austral winter and spring, respectively, whereas the diatom contribution was consistently <5%. They identified prasinophytes (*Pyramimonas* spp.) and chrysophytes (*Distenphenus speculum*) as the dominant nanoflagellate taxa with cryptophytes (*Cryptomonas* spp.) also abundant.

[30] The microphytoplankton routinely accounted for <30% (median: 15%) of total chl (Figure 2a) during FeCycle. Although members of this size class were not enumerated sensu stricto as part of each budget event, their relative taxonomic contribution was determined. Whereas dinoflagellates accounted numerically for ~70% of the microphytoplankton during budget events 1 and 3, the diatoms *Pseudo-nitzschia* spp. and *Chaetoceros* spp. were dominant during budget event 2 (data not shown).

[31] During FeCycle, total chl increased in increments of 15–30% between each budget sampling event ($P < 0.05$) from an initial level of 0.37 mg chl *a* m^{-3} to 0.63 mg chl *a* m^{-3} 5 days later (Figure 2a). The increase in chl appeared to be driven, at least following budget event 2, by chl associated with cells <2 μm ($P < 0.05$). Episodic increases in chl of this magnitude have been detected during previous years for this region from archived OCTS and SeaWiFs remote-sensing ocean color data [*Boyd et al.*, 2004b]. Analysis of MODIS-AQUA satellite data showed water masses adjacent to the FeCycle patch containing elevated levels of chl, at times >1 mg m^{-3} later in the study (P. L. Croot, unpublished data, 2005). There was also evidence that the SF_6-infused patch entrained adjacent water as it increased in size to ~400 km^2 over the duration of FeCycle (P. L. Croot, unpublished data, 2005). Thus advection of chl from an adjacent water mass into the FeCycle patch was a likely explanation for the observed increase in chl.

3.3. Primary Production and Iron Uptake

[32] Total primary production during each budget event generally decreased with increasing depth (Figure 3). Rates of production were mainly constant within the upper 12 m but thereafter declined through the mixed layer. Absolute rates of production in surface waters varied, with the highest rates measured during budget events 1 and 3 (Figures 3a and 3c). Despite differences in absolute rates of surface production, rates measured near the bottom of the seasonal mixed layer (45 m) were uniformly low (mean = 2.3 ± 1.1 mmol C m^{-3} d^{-1}). Measurements of size-fractionated phytoplankton primary production were not made on replicate samples; however, their pooled rates agreed well with total production. Size-fractionated production was generally dominated by the picoplankton, which accounted for between 27 and 66% of cumulative production (mean: 48 ± 11%).

[33] Consistent with their high biomass, the picoplankton were the dominant size fraction contributing to ^{55}Fe uptake during FeCycle, consistently contributing >50% of total Fe uptake near the surface and between 70 and 95% at depths >20 m (Figure 4). Marked differences in absolute rates of ^{55}Fe uptake between budget event days were not evident. Rates of ^{55}Fe uptake were ~7 times higher near the surface than rates measured near the bottom of the seasonal mixed layer (Figure 4). Consistent with this observation, *Maldonado et al.* [2005] showed that light-dependent uptake of Fe complexed to in situ ligands or EDTA

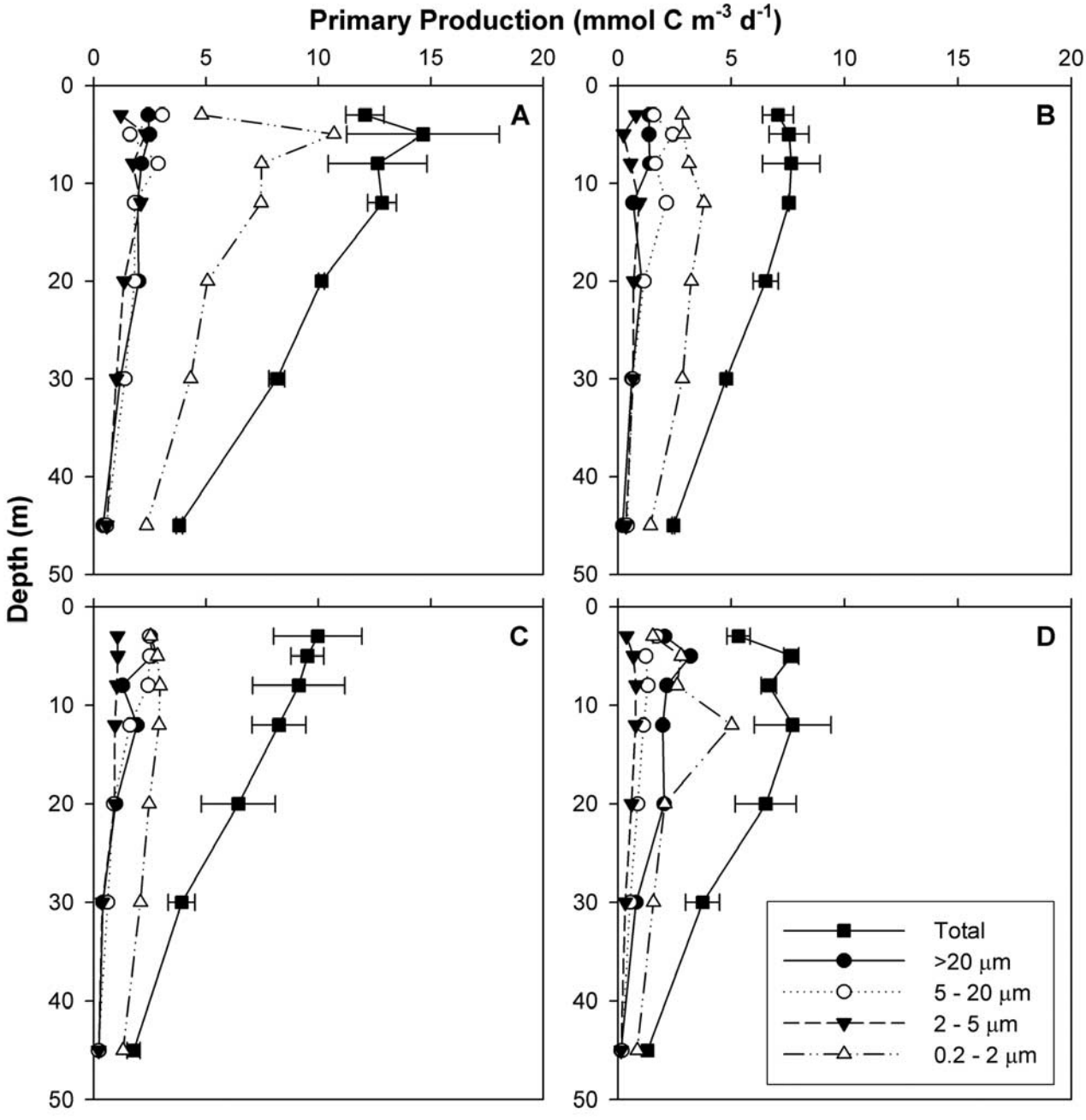

Figure 3. Mixed layer vertical profiles of total and size-fractionated ^{14}C primary production. (a) budget event 1 (4 February), (b) budget event 2 (5 February), (c) budget event 3 (6 February), and (d) budget event 4 (9 February). Size fractions are: square, total; solid circle, >20 μm; open circle, 5–20 μm; solid triangle, 2–5 μm; open triangle, 0.2–2 μm.

proceeded at a rate ~7 times higher than ^{55}Fe uptake in the dark. Although the lower uptake rates may reflect an impaired physiological status of cells incubated under low light or darkness, the photolability of the Fe-complexing ligands must also be considered. Measuring rates of ^{55}Fe uptake from several nonphotolabile ligands, *Maldonado et al.* [2005] demonstrated only a twofold increase in light-dependent ^{55}Fe uptake compared to rates measured in darkness. Thus it appears that light-mediated reduction of organically complexed Fe may have been an important mechanism to increase Fe availability during FeCycle as reflected by the higher rates of ^{55}Fe uptake measured for bottles deployed near the surface.

[34] Stoichiometric ^{55}Fe:^{14}C uptake ratios were calculated for both total plankton and individual size fractions (Figure 5). Although uptake ratios are not necessarily the same as steady state Fe:C ratios, *Twining et al.* [2004] recently demonstrated that radioisotope and stable metal

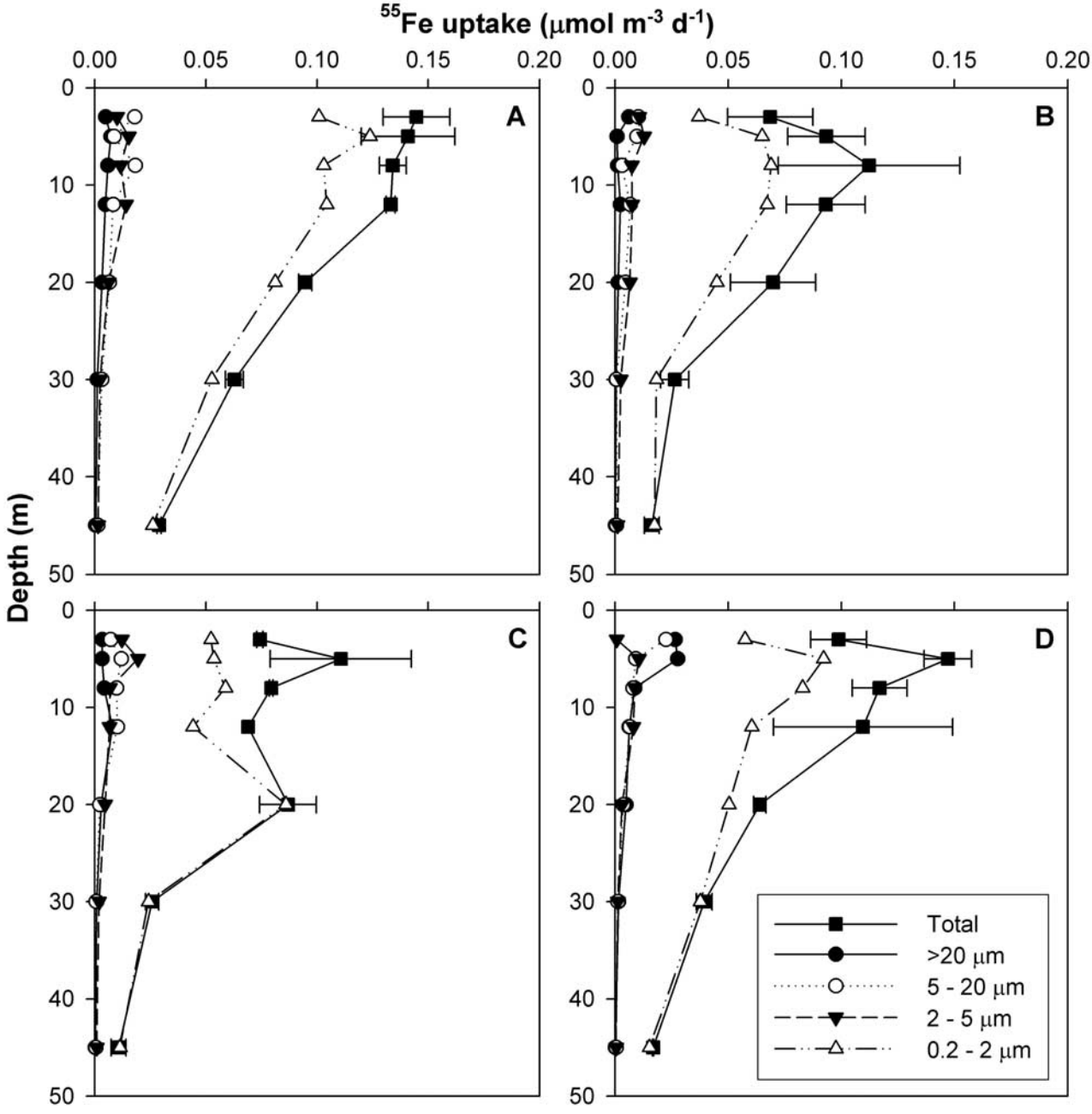

Figure 4. Mixed layer vertical profiles of total and size-fractionated ^{55}Fe uptake. (a) budget event 1 (4 February), (b) budget event 2 (5 February), (c) budget event 3 (6 February), and (d) budget event 4 (9 February). Symbols are as for Figure 5.

analyses are in good agreement when realistic tracer levels of ^{55}Fe are added as in FeCycle. Unlike primary production and ^{55}Fe uptake, total ^{55}Fe:^{14}C uptake ratios showed little depth-resolved variability with the ratios ranging between 5.5 and 19 μmol:mol (median: 10.5). Among size fractions, the picoplankton had the highest uptake ratios ranging from 6.5 to 37 μmol Fe:mol C (median: 17). This was consistent with the mean picoplankton ^{55}Fe:^{14}C uptake ratio of 25.3 ± 6.8 μmol:mol from unfertilized polar HNLC waters prior to the SOFeX Fe fertilization experiment [*Twining et al.*, 2004]. Other studies have similarly demonstrated that the picoplankton, in particular, the cyanobacterial component, have higher Fe requirements compared to larger size classes [e.g., *Brand*, 1991]. The average ^{55}Fe:^{14}C uptake ratio from the pooled remaining size fractions from FeCycle was ~5 μmol:mol. This was slightly lower than the radioisotope uptake results reported by *Twining et al.* [2004] for comparable size fractions. From their study, a mean pre-Fe fertilization Fe:C ratio of ~19 was derived for the nanoplankton and ~9 for the microphytoplankton. They also used a synchrotron X-ray fluorescence microprobe to resolve stable isotope-based Fe quotas of individual taxa

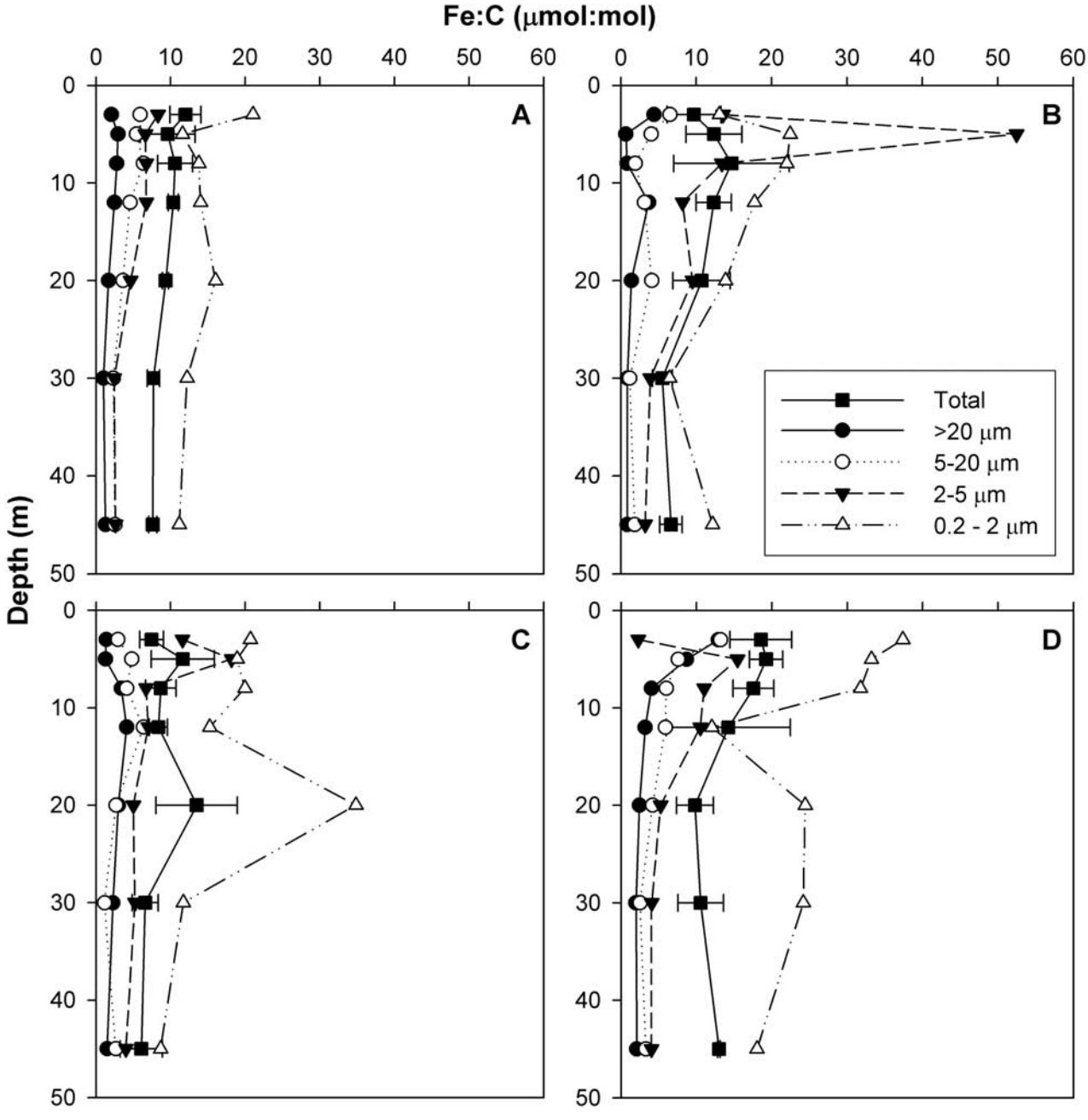

Figure 5. Mixed layer vertical profiles of total and size-fractionated ^{55}Fe:^{14}C uptake ratios (μmol:mol). (a) budget event 1 (4 February), (b) budget event 2 (5 February), (c) budget event 3 (6 February), and (d) budget event 4 (9 February). Symbols are as for Figure 5.

during SOFeX. Resolving Fe:C ratios of diatoms, autotrophic flagellates and heterotrophic flagellates, they reported values of 6.0, 8.7 and 14.1 μmol Fe: mol C, respectively, for polar HNLC waters [*Twining et al.*, 2004].

[35] Total ^{55}Fe uptake during FeCycle was also measured during short-term (6 hours) incubations. Rates of ^{55}Fe uptake were similar during both early morning and evening incubations but were ~30% higher at midday ($P < 0.001$). Compared to the 24-hour in situ deployments conducted during the budget events, short-term ^{55}Fe uptake rates were ~2 times higher. This may be due to the use of a higher concentration of Fe (2 nmol kg^{-1}) during the short-term uptake experiments [cf. *Twining et al.*, 2004] or to incubation under an overall higher irradiance (30% I_0 compared to a broad range of irradiances associated with the depth-resolved incubations). Also as part of the diel sampling events, PE experiments were conducted (Table 1). Whereas the rate of chl-normalized maximum photosynthesis (P_m) was relatively stable, varying by no more than 25% over a diel cycle,

Table 1. Photosynthesis Versus Irradiance and Short-Term ^{55}Fe Uptake Rates: Diel Sampling (±S.D.)

	Diel Cycle (7 February)				Diel Cycle (11 February)				
Parameter	Event 1 (0600 LT)	Event 2 (1200 LT)	Event 3 (1600 LT)	Event 4 (2100 LT)	Event 1 (0200 LT)	Event 2 (0700 LT)	Event 3 (1200 LT)	Event 4 (1600 LT)	Event 5 (2000 LT)
P_m, g C g chl^{-1} h^{-1}	2.65	2.3	2.61	2.03	1.31	1.91	3.62	2.55	2.91
α, (g C g chl^{-1} h^{-1})/(μmol m^{-2} s^{-1})	2×10^{-2}	1.6×10^{-2}	1.1×10^{-2}	0.7×10^{-2}	1.1×10^{-2}	1.3×10^{-2}	1.9×10^{-2}	0.9×10^{-2}	3.1×10^{-2}
^{55}Fe uptake, μmol m^{-3} d^{-1}	n.d.[a]	n.d.	n.d.	n.d.	n.d.	0.28 (3×10^{-3})	0.36 (2×10^{-3})	0.29 (2×10^{-3})	n.d.

[a]Not determined.

P_m increased by a factor of 2 from dawn to post-midday sampling times.

3.4. Iron Status of the Endemic Phytoplankton Community

3.4.1. Indices of Iron Deficiency

[36] F_v/F_m measured on phytoplankton during FeCycle was consistently low (< 0.25) suggesting Fe deficiency (Table 2). Comparable low values of F_v/F_m have been previously reported for communities co-limited by silicic acid and Fe [*Hutchins et al.*, 2001] and for other HNLC regimes dominated by picophytoplankton [*Boyd*, 2002; *Sosik and Olson*, 2002] including HNLSiLC SA waters in the vicinity of the FeCycle site [*Boyd et al.*, 1999]. By comparison, F_v/F_m is >0.6 in nutrient-replete phytoplankton [*Kolber and Falkowski*, 1993].

[37] Considering only the picophytoplankton, our measurements of cellular chl and F_v/F_m appear to be in conflict. Whereas the consistently low F_v/F_m was a sign of chronic Fe deficiency, concomitant increases in chl cell^{-1} during FeCycle did not support this characterization. Cyanobacteria can present problems in the measurement and interpretation of variable fluorescence resulting in generally lower values for F_v/F_m compared to eukaryotes [*Campbell et al.*, 1998]. The use of FRRF, however, has been validated for common cyanobacteria (e.g., *Synechococcus* spp., *Prochlorococcus* spp.) that are dominant in open ocean waters [*Behrenfeld and Kolber*, 1999].

[38] A Fd Index ([Fd]/[Fd + Flvd]) was also determined for the diatom component of the microplankton. Whereas Fe-sufficient phytoplankton typically have a Fd Index ≅ 1 [*Xia et al.*, 2004], during FeCycle, the Fd Index of the microplankton diatoms was <0.2 (Tables 2 and 3). When considered together with F_v/F_m measured for this size fraction (Table 3), this was suggestive of a Fe-deficient status for diatoms.

[39] Several microphytoplankton samples were processed for determination of their internal Fe quotas. Sampling coincided with the occurrence of a numerically dominant (72–85%) assemblage of the diatom *Pseudo-nitzschia* spp. occuring at the study site. Consistent with the surplus N measured in the SF_6-labeled patch, molar C:N ratios ranged between 6.8 and 7.3 (not shown). Fe:C ratios were variable, ranging between 30.2 and 82.3 μmol:mol (median: 33 μmol:mol) (Table 3). By comparison, the average ^{55}Fe:^{14}C uptake ratio measured at 12 m and 20 m depth for the microplankton earlier in the study was 3.1 ± 1.1 μmol:mol, a difference of an order of magnitude. *Twining et al.* [2004] presented a mean Fe:C ratio for diatoms of 6 μmol:mol prior to Fe fertilization with a fourfold increase in Fe:C following fertilization. The relatively high Fe:C ratios associated with the microplankton measured during FeCycle were thus more similar to what might be expected following an infusion of Fe to the patch, such as a dust event, yet these ratios were not consistent with the low F_v/F_m and Fd Index ratios presented. Several possibilities exist to explain this apparent discrepancy. Constitutive expression of Flvd [*McKay et al.*, 2000] would result in a depressed Fd Index, although this would have little impact on F_v/F_m. A temporal lag between the acquisition of Fe and corresponding increases in F_v/F_m and the Fd Index could also explain the discrepancy.

3.4.2. Iron Perturbation Experiment

[40] Analyses at the start of the Fe perturbation experiment initiated on 3 February confirmed the prior characterization of the study site as a SA HNLSiLC water mass (see auxiliary material[1]). Concentrations of silicic acid and phosphate did not vary between Fe-, or DFB-amended bottles and controls following 72-hour incubation ($P > 0.05$) (auxiliary material). By contrast, levels of nitrate decreased by 11% in the Fe-amended treatment, but not in bottles amended with DFB relative to the controls ($P < 0.05$), suggesting that Fe addition to the enclosed assemblage stimulated nitrate utilization only.

[41] Concomitant with the depletion of nitrate was a modest increase in total chl *a* in Fe-amended bottles ($P < 0.05$) but not in bottles to which DFB was added ($P > 0.05$) (Figure 6a). All size fractions, except the 2–5 μm nanoplankton, contributed to the increase in chl *a* ($P < 0.05$) (Figure 6b). Size-fractionated chl *a* from the DFB-treated bottles did not vary from the controls ($P > 0.05$) (Figure 6b). Fe addition also resulted in a modest increase of F_v/F_m

Table 2. Physiological Indices of Cellular Fe Status (±S.D.)

	Budget Event			
Parameter	Event 1 (4 Feb)	Event 2 (5 Feb)	Event 3 (6 Feb)	Event 4 (9 Feb)
fg chl *a* cell^{-1}[a]	0.59 (2×10^{-1})	1.4 (2×10^{-1})	1.2 (2×10^{-1})	1.7 (9×10^{-2})
F_v/F_m	0.24 (7×10^{-3})	0.22 (0)	0.22 (2×10^{-3})	0.2 (9×10^{-3})
Fd Index[b]	n.d.[c]	0.17 (0.1)	0.18 (0.1)	n.d.

[a]Determined for picophytoplankton only.
[b]Determined for microphytoplankton only.
[c]Not determined.

[1]Auxiliary material is available at ftp://ftp.agu.org/apend/gb/2005GB002482.

Table 3. Physiological Indices of Cellular Fe Status: Diel Sampling (±S.D.)

	Diel Cycle (7 February)				Diel Cycle (11 February)				
Parameter	Event 1 (0600 LT)	Event 2 (1200 LT)	Event 3 (1600 LT)	Event 4 (2100 LT)	Event 1 (0200 LT)	Event 2 (0700 LT)	Event 3 (1200 LT)	Event 4 (1600 LT)	Event 5 (2000 LT)
fg chl *a* cell^{-1}[a]	1.1 (1×10^{-1})	1.6 (1×10^{-2})	1.6 (1×10^{-1})	1.2 (1×10^{-2})	3 (1×10^{-1})	0.69 (2×10^{-1})	0.31 (6×10^{-2})	0.51 (2×10^{-1})	1.2 (2×10^{-1})
F_v/F_m	0.22 (6×10^{-3})	0.21 (2×10^{-3})	0.17 (2×10^{-2})	0.22 (5×10^{-3})	0.22 (3×10^{-3})	0.2 (5×10^{-3})	0.17 (2×10^{-3})	0.18 (4×10^{-3})	0.24 (5×10^{-3})
F_v/F_m (micro PP)	n.d.[b]	n.d.	n.d.	n.d.	0.27 (1.4×10^{-2})	n.d.	0.23 (7×10^{-3})	0.26 (8×10^{-3})	0.22 (3×10^{-3})
Fd Index[c]	n.d.	n.d.	n.d.	n.d.	0.12 (0)	n.d.	0.15 (0)	0.1 (0.1)	n.d.
Fe:C, μmol:mol	n.d.	n.d.	n.d.	n.d.	33 (2.7)	n.d.	82.3 (87.3)	n.d.	30.2 (7.5)

[a]Determined for picophytoplankton only.
[b]Not determined.
[c]Determined for microphytoplankton only.

relative to the controls ($P < 0.05$) (Figure 6c). Similar results for total chl and F_v/F_m were obtained with both perturbation experiments.

[42] Fe-responsive increases of both chl *a* and F_v/F_m became saturated at a low level (~0.5 nmol kg^{-1}) addition of Fe. By contrast, reducing Fe availability via DFB addition did not appear to increase physiological Fe stress, suggesting that the endemic phytoplankton community was severely Fe deficient.

[43] Use of DFB to withhold Fe from the endemic phytoplankton community was validated in a companion study where Fe uptake was measured using a variety of model ligands [*Maldonado et al.*, 2005]. Although some Fe complexed to DFB was acquired by all size fractions of phytoplankton, rates of Fe uptake measured from ^{55}Fe-DFB were only ~1% compared to Fe complexed to other ligands tested [*Maldonado et al.*, 2005].

3.5. A Phytoplankton Iron Budget

[44] The picoplankton size fraction comprised the single largest pool of biogenic Fe measured during FeCycle (Table 4). On the basis of Fe:C ratios derived from ^{55}Fe and ^{14}C uptake measurements, we calculated that >93% of biogenic Fe was associated with the picoplankton. Within the picoplankton size fraction, the heterotrophic bacteria and the cyanobacteria each contributed ~43% of this Fe. This roughly equal contribution was derived, however, by applying the same Fe:C ratio (18.5 μmol:mol; Fe:C uptake mean for picoplankton incubated at 12 m and 20 m depths) to each group. By applying a bacterial-specific ratio of 7.5 μmol Fe: mol C appropriate for Fe-deficient waters to the heterotrophs [*Tortell et al.*, 1996], the bacterial contribution to the biological Fe pool decreased to ~25 nmol m^{-3}, or <20% of total picoplankton Fe. Thus, depending on the Fe:C ratio applied, the picophytoplankton contributed between 58% and 82% of picoplankton biogenic Fe and consistently >90% of total phytoplankton biogenic Fe.

[45] We calculated algal Fe demand, derived from our measurement of size-fractionated ^{55}Fe uptake, to be greatest among the picoplankton size fraction, accounting for ~80% of total Fe demand. An assessment of steady state Fe demand compiled in a companion study [*Strzepek et al.*, 2005] further predicted the cyanobacteria to account for ~90% of total Fe demand within the picoplankton size fraction. This was despite the observation that both the cyanobacteria and the heterotrophic picoplankton contributed equally to biomass during FeCycle (Table 4).

[46] Regeneration of Fe was derived from direct measurements made from grazing experiments conducted during FeCycle [*Strzepek et al.*, 2005]. Roughly equal rates of Fe regeneration were measured from the heterotrophic bacteria and the picophytoplankton during the grazing experiments. Considering only Fe regenerated by herbivory, we estimate that ~20% of total algal Fe demand was satisfied. This value increased to ~40% if we considered also Fe regenerated by bacterivory.

[47] Regeneration of Fe from phytoplankton represents an important nutrient flux in oligotrophic regions [*Hutchins et al.*, 1993]. Both grazing and viral lysis [*Gobler et al.*, 1997; *Poorvin et al.*, 2004] have been demonstrated to mediate the regeneration of Fe from phytoplankton. Considering a regeneration efficiency ([Fe excreted/Fe ingested] × 100) approximating 70% for grazing by mixotrophic nanoflagellates [*Maranger et al.*, 1998] and heterotrophic microflagellates [*Chase and Price*, 1997] and between 75 and 95% for metazoan grazers [*Hutchins et al.*, 1995], grazing-mediated regeneration of Fe was expected to contribute substantially to the cycling of Fe during FeCycle. Several reports demonstrate grazing pressure to be high in SA waters [*Hall et al.*, 1999, 2004], particularly on the picophytoplankton. During the summer, rates of growth and grazing are balanced for this group [*Hall et al.*, 2004], as has been demonstrated for other HNLC regions [*Landry et al.*, 1997]. Depending on the season, nanoflagellates and microzooplankton graze between 45 and 80% of picophytoplankton standing crop, and consistently ~100% of picoplankton primary production in SA waters [*Hall et al.*, 1999, 2004]. Grazing thus represents the major pathway by which picoplankton biomass is transferred to higher trophic levels in this region.

[48] Grazing trials conducted during FeCycle confirmed the high rates of grazing upon picophytoplankton previously reported for SA waters [*Strzepek et al.*, 2005]. More striking, however, was the demonstration of apparent differential regeneration of Fe from phytoplankton and bacterial prey sources. When grazers were presented ^{55}Fe-labeled

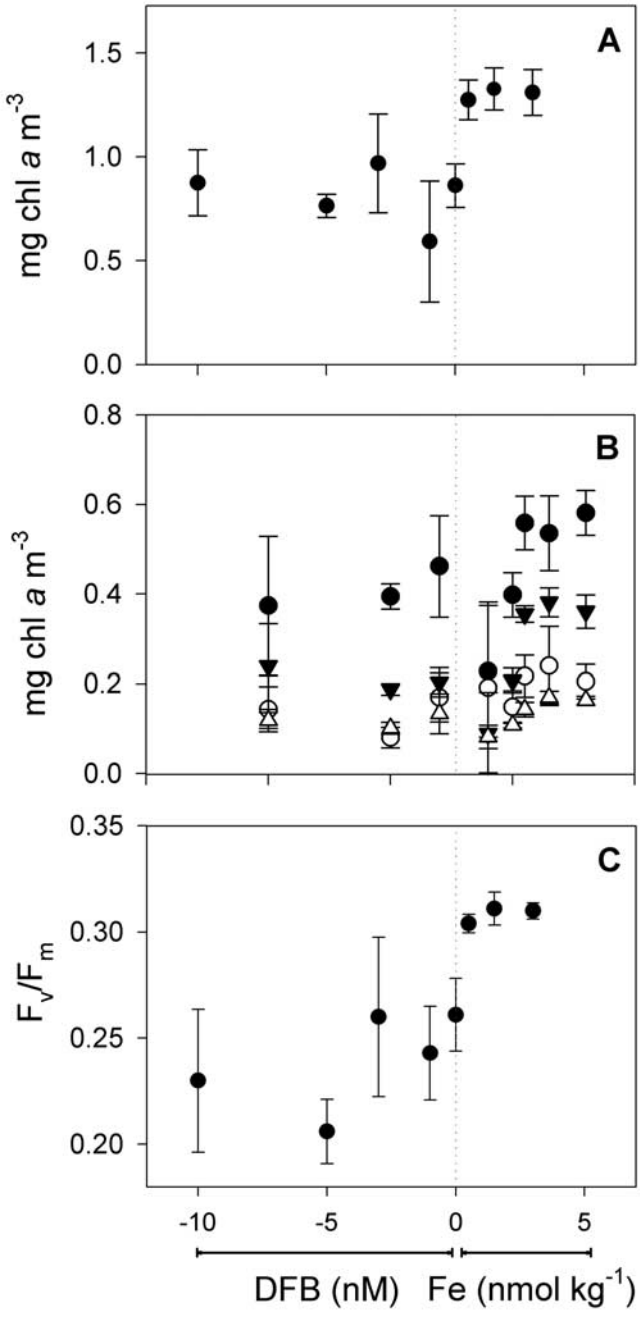

Figure 6. (a) Total and (b) size-fractionated chl and (c) F_v/F_m following 72-hour on-deck incubation initiated on 3 February. Results are the means ± SD of triplicate incubations. Molar additions of DFB are plotted as negative values in recognition of the ability of DFB to withhold Fe from phytoplankton. Dashed line: control (no addition). Size fractions: open triangle, 20 μm; solid triangle, 5–20 μm; open circle, 2–5 μm; solid circle, 0.2–2 μm.

bacteria (0.2–0.8 μm size fraction) as prey, >90% of the liberated Fe was partitioned to the dissolved fraction following the 24-hour grazing trial [*Strzepek et al.*, 2005]. In contrast, when ^{55}Fe-labeled phytoplankton (0.8–8 μm size fraction) were presented as prey, only 25% of the Fe was regenerated into the dissolved phase. Does this imply that Fe regenerated from the heterotrophic bacteria was somehow more refractory than that regenerated from the picophytoplankton and thus unavailable for uptake by ungrazed plankton remaining in the trials? Consistent with this idea, *Twiss and Campbell* [1995] reported that microzooplankton grazing on radiolabeled picoplankton prey resulted in release of metals into the dissolved organic matter pool in forms that were less available for resorption by remaining ungrazed *Synechococcus*. Organic complexation of the regenerated metals, they argued, may serve to prolong their residence times in the water column. By contrast, >50% of the Fe contained in ^{59}Fe-labeled diatom prey grazed by the copepod *Acartia tonsa* was partitioned to the dissolved pool within 5 hours of being consumed [*Hutchins et al.*, 1995].

[49] A caveat associated with the budget was our treatment of the nanoplankton size fraction. The budget includes only biomass estimates for the nanophytoflagellate component. Further, we applied to the nanophytoflagellates, the same Fe regeneration factor derived from grazing experiments for phytoplankton in the size range 0.8–8 μm [*Strzepek et al.*, 2005], despite this group encompassing the size range 2–20 μm. Not included in our budget was Fe contributed by diatoms associated with the nanoplankton size fraction. Diatoms associated with this size fraction were enumerated on only one occasion during FeCycle and were $<5 \times 10^7$ cells m^{-3} [*Leblanc et al.*, 2005], nearly 20-fold lower than the combined nanophytoflagellate component (Figure 2b). Applying a mean diatom biomass estimate of 0.024 mmol C m^{-3} for SA waters [*Bradford-Grieve et al.*, 1997] combined with the nanoplankton Fe:C ratio derived for FeCycle (Table 4), it is clear that negligible biogenic Fe (~0.1 nmol m^{-3}) was associated with diatoms of this size class. If we further consider that diatoms are generally subject to less intensive grazing pressure compared to picophytoplankton in HNLC systems [*Landry et al.*, 1997] and that diatoms are preferentially removed relative to other phytoplankton from the mixed layer by sinking [*Dugdale et al.*, 1995; *Buesseler*, 1998], then it is clear that regeneration of Fe from nanoplankton-sized diatoms was likely of minor importance during FeCycle. This view is consistent with the low suspended biogenic silica content measured in the FeCycle study patch during the budget events (0.07 ± 0.02 mmol m^{-3}) and the lower flux (75–127 μmol m^{-2} d^{-1}) of biogenic silica exported during FeCycle (Frew et al., submitted manuscript, 2005) relative to previous measurements made in the general vicinity [*Nodder and Northcote*, 2001].

[50] Our budget also did not take into account an elevated Fe pool associated with the microphytoplankton size fraction measured over the course of a diel cycle on 11 February and which is included in Table 4 for comparative purposes. When included in our calculations, this sample, in which the diatom *Pseudo-nitszchia* spp. was numerically dominant, accounted for ~22% of the total phytoplankton Fe pool. The increase in the diatom component of the phytoplankton biogenic Fe pool was consistent with a >4-fold increase ($P < 0.005$), compared to the budget events, in suspended biogenic silica to 0.32 ± 0.03 mmol m^{-3} coinciding with

Table 4. A Fe Budget Comprising Phytoplankton Size Fractions and Major Functional Groups (±S.D.)

Plankton Group	Biomass, mmol C m^{-3}	Fe:C, μmol:mol	Biogenic Fe, nmol m^{-3}	Particulate Fe, nmol m^{-3}	Fe Demand, nmol m^{-3} d^{-1}	Fe Regeneration, nmol m^{-3} d^{-1}
0.22–2 μm	7.8 (3.1)	18.5 (4.5)	144.3 (92.4)	130 (30)	67.3 (17.5)	
Bacteria	3.3 (2)	18.5 (4.5)	61.1 (51.9)	n.d.	1.4	15
PCyano	3.4 (0.8)	18.5 (4.5)	62.9 (30.1)	n.d.	22.2 –84.6	16.5
PEuk	1.1 (0.3)	18.5 (4.5)	20.4 (10.5)	n.d.	1.8 –9.9	
2–20 μm (NF)	1.2 (0.5)	5.7 (1.1)	6.8 (4.2)	290 (180)	13.3 (3.1)	1.6
NPF	0.9 (0.4)	5.7 (1.1)	5.1 (3.3)	n.d.	n.d.	
NHF	0.3 (0.1)	5.7 (1.1)	1.7 (0.9)	n.d.	n.d.	
>20 μm	1.3 (0.1)	2.7 (0.6)	3.5 (1)	330 (100)	4.3 (1.7)	
Net plankton	1.3 (0.1)	33 (3)	42.9 (7.2)	n.d.	n.d.	
Σ					84.9 (22.3)	33.1

sampling on 11 February. Applying mesozooplankton grazing estimates from HNLC waters (0.25–0.88 d^{-1}) [*Roman and Gauzens*, 1997] as well as estimates of regeneration efficiency (0.88 d^{-1}) and fractionation of labile metal (0.31 d^{-1}) (M. R. Twiss, personal communication, 2005) to this pool, we propose an additional 5–10 nmol m^{-3} d^{-1} of labile Fe could be regenerated from the microphytoplankton.

[51] An additional pool of Fe that may have contributed to phytoplankton Fe demand during FeCycle was the lithogenic fraction of particulate Fe (Fe_p). Overall, between 72 and 98% of the Fe_p pool was lithogenic, the highest proportion being associated with the >20 μm size fraction (Table 4) (Frew et al., submitted manuscript, 2005). In contrast, the entirety of the 0.2–2 μm Fe_p pool could be accounted for by biogenic Fe associated with the picoplankton.

[52] It has been recognized for some time that phytoplankton can use particulate and colloidal Fe, although the efficacy with which they do so is thought to be dependent on the thermodynamic and photochemical stability of the various Fe species [*Rich and Morel*, 1990]. Exceptions to this are the heterotrophic and mixotrophic flagellates that are able to effect dissolution of inorganic particles through phagotrophy [*Barbeau et al.*, 1996; *Nodwell and Price*, 2001] and possibly specialized reducing microenvironments such as buoyant diatom mats or *Trichodesmium* colonies [*Rueter et al.*, 1992]. The design of the grazer experiments conducted during FeCycle precluded us from reliably estimating the contributions of Fe regenerated from the lithogenic Fe_p pool to phytoplankton Fe demand since these trials tracked ^{55}Fe-labeled prey and not total Fe. Considering that Fe_p contributed by atmospheric deposition was probably the major source of new Fe introduced into the study patch [*Boyd et al.*, 2005], dissolution of the lithogenic Fe_p pool may have been an additional source of new Fe to phytoplankton. This suggestion was supported by the results of Frew et al. (submitted manuscript, 2005), who found that lithogenic Fe can be converted to biogenic Fe in the mixed layer with modest efficiency (~50%) and over short timescales of weeks to months.

4. Conclusions

[53] An attempt to construct a budget showing the flux of Fe through size-fractionated phytoplankton pools demonstrated that the picophytoplankton comprised the dominant phytoplankton size fraction in terms of abundance, chl, carbon biomass and primary production. Consistent with this, the picophytoplankton also comprised the dominant pool of biogenic Fe during FeCycle, containing >90% of total phytoplankton Fe. Using grazing rates presented by *Strzepek et al.* [2005], we estimated that regeneration of Fe by herbivory was able to satisfy ~20% of the algal Fe demand and that this increased to ~40% if we also included bacterivory. Estimates of maximum Fe regeneration by this mechanism were sufficient to account for between 29 and 77% of the algal Fe demand. Viral lytic activity, which was not considered in the budget, was expected to account for additional regeneration of Fe as reported by *Strzepek et al.* [2005]. New Fe input into the FeCycle study site was predominantly as particulate Fe delivered most likely from atmospheric sources. Accounting for solubilization and remobilization of lithogenic Fe_p, either through chemical or biological reductive mechanisms, lithogenic Fe_p provided an additional minor source of Fe_d to the algal community. Overall, the evidence supported an algal assemblage whose production was supported mainly by regenerative processes during FeCycle with a calculated "*fe*" ratio (uptake of new Fe/uptake of new + regenerated Fe) of 0.09 [*Boyd et al.*, 2005]. Yet, the inability of our measured regenerative processes (herbivory and bacterivory) to completely account for algal Fe demand was consistent with the chronic Fe deficiency observed in this system.

[54] **Acknowledgments.** This material is based upon work supported by the New Zealand PGSF Ocean Ecosystems Programme (P. W. B.) and by the U.S. National Science Foundation under grant numbers OISE-0238615 (R. M. L. M.), OISE-0236987 (D. A. H.) and OISE-0240092 and ANT-0228895 (S. W. W.). We thank the officers and crew on the NIWA R/V *Tangaroa*, the personnel at NIWA vessel services and the entire FeCycle team for their cooperation both during the study and post-cruise with analysis and interpretation of data. Special thanks are extended to S. Sañudo-Wilhelmy, A. Tovar-Sanchez, M. Oliver, A. Cumming, C. Hare, K. Leblanc and J. Higgins for their assistance with field sampling and data analysis.

References

Banse, K. (1996), Low seasonality of low concentrations of surface chlorophyll in the subantarctic water ring: Underwater irradiance, iron, or grazing?, *Prog. Oceanogr.*, *37*, 241–291.

Banse, K., and D. C. English (1997), Near-surface phytoplankton pigment from the Coastal Zone ColorScanner in the Subantarctic region southeast of New Zealand, *Mar. Ecol. Prog. Ser.*, *156*, 51–66.

Barbeau, K., J. W. Moffett, D. A. Caron, P. L. Croot, and D. L. Erdner (1996), Role of protozoan grazing in relieving iron limitation of phytoplankton, *Nature*, *380*, 61–64.

Behrenfeld, M. J., and Z. S. Kolber (1999), Widespread iron limitation of phytoplankton in the South Pacific Ocean, *Science*, *283*, 840–843.

Booth, B. C. (1988), Size classes and major taxonomic groups of phytoplankton at two locations in the subarctic Pacific Ocean in May and August, 1984, *Mar. Biol.*, *97*, 275–286.

Bowie, A. R., M. T. Maldonado, R. D. Frew, P. L. Croot, E. P. Achterberg, R. F. C. Mantoura, P. J. Worsfold, C. S. Law, and P. W. Boyd (2001), The fate of added iron during a mesoscale fertilisation experiment in the Southern Ocean, *Deep Sea Res., Part II*, *48*, 2703–2743.

Boyd, P. W. (2002), Environmental factors controlling phytoplankton processes in the Southern Ocean, *J. Phycol.*, *38*, 844–861.

Boyd, P. W., and P. J. Harrison (1999), Phytoplankton dynamics in the NE subarctic Pacific, *Deep Sea Res., Part II*, *46*, 2405–2432.

Boyd, P., J. LaRoche, M. Gall, R. Frew, and R. M. L. McKay (1999), Role of iron, light and silicate in controlling algal biomass in subantarctic waters SE of New Zealand, *J. Geophys. Res.*, *104*, 13,395–13,408.

Boyd, P. W., et al. (2000), A mesoscale phytoplankton bloom in the polar Southern Ocean stimulated by iron fertilization, *Nature*, *407*, 695–702.

Boyd, P. W., et al. (2004a), The decline and fate of an iron-induced subarctic phytoplankton bloom, *Nature*, *428*, 549–553, doi:10.1038/nature02437.

Boyd, P. W., G. McTainsh, V. Sherlock, K. Richardson, S. Nichol, M. Ellwood, and R. Frew (2004b), Episodic enhancement of phytoplankton stocks in New Zealand subantarctic waters: Contribution of atmospheric and oceanic iron supply, *Global Biogeochem. Cycles*, *18*, GB1029, doi:10.1029/2002GB002020.

Boyd, P. W., et al. (2005), FeCycle: Attempting an iron biogeochemical budget from a mesoscale SF6 tracer experiment in unperturbed low iron waters, *Global Biogeochem. Cycles*, doi:10.1029/2005GB002494, in press.

Bradford-Grieve, J. M., F. H. Chang, M. Gall, S. Pickmere, and F. Richards (1997), Size-fractionated phytoplankton standing stocks and primary production during austral winter and spring 1993 in the Subtropical Convergence region near New Zealand, *N. Z. J. Mar. Freshwater Res.*, *31*, 201–224.

Bradford-Grieve, J. M., P. W. Boyd, F. H. Chang, S. Chiswell, M. Hadfield, J. A. Hall, M. R. James, S. D. Nodder, and E. A. Shuskina (1999), Pelagic ecosystem structure and functioning in the Subtropical Front region east of New Zealand in austral winter and spring 1993, *J. Plankton Res.*, *21*, 405–428.

Brand, L. E. (1991), Minimum iron requirements of marine phytoplankton and the implications for the biogeochemical control of new production, *Limnol. Oceanogr.*, *36*, 1756–1771.

Buesseler, K. O. (1998), The decoupling of production and particulate export in the surface ocean, *Global Biogeochem. Cycles*, *12*, 297–310.

Campbell, D., V. Hurry, A. K. Clarke, P. Gustafsson, and G. Öquist (1998), Chlorophyll fluorescence analysis of cyanobacterial photosynthesis and acclimation, *Microbiol. Mol. Biol. Rev.*, *62*, 667–683.

Cavendar-Bares, K. K., E. L. Mann, S. W. Chisholm, M. E. Ondrusek, and R. R. Bidigare (1999), Differential response of equatorial Pacific phytoplankton to iron fertilization, *Limnol. Oceanogr.*, *44*, 237–246.

Chang, F. H. (1988), Distribution, abundance, and size composition of phytoplankton off Westland, New Zealand, February 1982, *N. Z. J. Mar. Freshwater Res.*, *22*, 345–367.

Chang, F. H., and M. Gall (1998), Phytoplankton assemblages and photosynthetic pigments during winter and spring in the Subtropical Convergence region near New Zealand, *N. Z. J. Mar. Freshwater Res.*, *32*, 515–530.

Chase, Z., and N. M. Price (1997), Metabolic consequences of iron deficiency in heterotrophic marine protozoa, *Limnol. Oceanogr.*, *42*, 1673–1684.

Coale, K. H., et al. (1996), A massive phytoplankton bloom induced by an ecosystem-scale iron fertilization experiment in the equatorial Pacific Ocean, *Nature*, *383*, 495–501.

Dugdale, R. C., F. P. Wilkerson, and H. J. Minas (1995), The role of a silicate pump in driving new production, *Deep Sea Res., Part I*, *42*, 697–719.

Eldridge, M. L., C. G. Trick, M. B. Alm, G. R. DiTullio, E. L. Rue, K. W. Bruland, D. A. Hutchins, and S. W. Wilhelm (2004), Phytoplankton community response to a manipulation of bioavailable iron in HNLC waters of the subtropical Pacific Ocean, *Aquat. Microb. Ecol.*, *35*, 79–91.

Fukuda, R., H. Ogawa, T. Nagata, and I. Koike (1998), Direct determination of carbon and nitrogen contents of natural bacterial assemblages in marine environments, *Appl. Environ. Microbiol.*, *64*, 3352–3358.

Fung, I. Y., S. K. Meyn, I. Tegen, S. C. Doney, J. G. John, and J. K. B. Bishop (2000), Iron supply and demand in the upper ocean, *Global Biogeochem. Cycles*, *14*, 281–295.

Gobler, C. J., D. A. Hutchins, N. S. Fisher, E. M. Cosper, and S. A. Sañudo-Wilhelmy (1997), Release and bioavailability of C, N, P, Se, and Fe following viral lysis of a marine chrysophyte, *Limnol. Oceanogr.*, *42*, 1492–1504.

Hall, J. A., M. R. James, and J. M. Bradford-Grieves (1999), Structure and dynamics of the pelagic microbial food web of the Subtropical Convergence region east of New Zealand, *Aquat. Microb. Ecol.*, *20*, 95–105.

Hall, J., K. Safi, and A. Cumming (2004), Role of microzooplankton grazers in the subtropical and subantarctic waters to the east of New Zealand, *N. Z. J. Mar. Freshwater Res.*, *38*, 91–101.

Horner, R. A. (2002), *A Taxonomic Guide to Some Common Marine Phytoplankton*, 195 pp., Biopress, London.

Hutchins, D. A., G. R. DiTullio, and K. W. Bruland (1993), Iron and regenerated production: Evidence for biological iron recycling in two marine environments, *Limnol. Oceanogr.*, *38*, 1242–1255.

Hutchins, D. A., W.-X. Wang, and N. S. Fisher (1995), Copepod grazing and the biogeochemical fate of diatom iron, *Limnol. Oceanogr.*, *40*, 989–994.

Hutchins, D. A., P. N. Sedwick, G. R. DiTullio, P. W. Boyd, F. B. Griffiths, B. Quéguiner, and A. C. Crossley (2001), Control of phytoplankton growth by iron and silicic acid availability in the subantarctic Southern Ocean: Experimental results from the SAZ project, *J. Geophys. Res.*, *106*, 31,559–31,572.

Kolber, Z. S., and P. G. Falkowski (1993), Use of active fluorescence to estimate phytoplankton photosynthesis in situ, *Limnol. Oceanogr.*, *38*, 1646–1665.

Landry, M. R., et al. (1997), Iron and grazing constraints on primary production in the central equatorial Pacific: An EqPac synthesis, *Limnol. Oceanogr.*, *42*, 405–418.

La Roche, J., H. Murray, M. Orellana, and J. Newton (1995), Flavodoxin expression as an indicator of iron limitation in marine diatoms, *J. Phycol.*, *31*, 520–530.

Laws, E. A. (1991), Photosynthetic quotients, new production and net community production in the open ocean, *Deep Sea Res.*, *38*, 143–167.

Leblanc, K., C. E. Hare, P. W. Boyd, K. W. Bruland, B. Sohst, S. Pickmere, M. C. Lohan, K. Buck, M. Ellwood, and D. A. Hutchins (2005), Fe and Zn effects on the Si cycle and diatom community structure in two contrasting high and low-silicate HNLC areas, *Deep Sea Res., Part I*, *52*, 1842–1864.

Li, W. K. W., P. M. Dickie, B. D. Irwin, and A. M. Wood (1992), Biomass of bacteria, cyanobacteria, prochlorophyte and photosynthetic eukaryotes in the Sargasso Sea, *Deep Sea Res.*, *39*, 501–519.

Maldonado, M. T., R. F. Strzepek, S. Sander, and P. W. Boyd (2005), Acquisition of iron bound to strong organic complexes, with different Fe binding groups and photochemical reactivities, by plankton communities in Fe-limited subantarctic waters, *Global Biogeochem. Cycles*, *19*, GB4S23, doi:10.1029/2005GB002481.

Maranger, R., D. F. Bird, and N. M. Price (1998), Iron acquisition by photosynthetic marine phytoplankton from ingested bacteria, *Nature*, *396*, 248–251.

McKay, R. M. L., J. La Roche, A. F. Yakunin, D. G. Durnford, and R. J. Geider (1999), Accumulation of ferredoxin and flavodoxin in a marine diatom in response to Fe, *J. Phycol.*, *35*, 510–519.

McKay, R. M. L., T. A. Villareal, and J. La Roche (2000), Vertical migration by Rhizosolenia spp. (Bacillariophyceae): Implications for Fe acquisition, *J. Phycol.*, *36*, 669–674.

Mioni, C. E., S. M. Handy, M. J. Ellwood, M. R. Twiss, R. M. L. McKay, P. W. Boyd, and S. W. Wilhelm (2005), Tracking changes in bioavailable Fe within high-nitrate low-chlorophyll oceanic waters: A first estimate using a heterotrophic bacterial bioreporter, *Global Biogeochem. Cycles*, doi:10.1029/2005GB002476, in press.

Nodder, S. D., and L. C. Northcote (2001), Episodic particulate fluxes at southern temperate mid-latitudes (42–45°S) in the Subtropical Front region, east of New Zealand, *Deep Sea Res., Part I*, *48*, 833–864.

Nodder, S. D., P. W. Boyd, S. M. Chiswell, M. H. Pinkerton, J. M. Bradford-Grieve, and M. Greig (2005), Temporal coupling between surface and deep-ocean biogeochemical processes in contrasting subtropical and subantarctic water masses, southwest Pacific Ocean, *J. Geophys. Res.*, doi:10.1029/2004JC002833, in press.

Nodwell, L. M., and N. M. Price (2001), Direct use of inorganic colloidal iron by marine mixotrophic phytoplankton, *Limnol. Oceanogr.*, *46*, 765–777.

Parekh, P., M. J. Follows, and E. Boyle (2004), Modeling the global iron cycle, *Global Biogeochem. Cycles*, *18*, GB1002, doi:10.1029/2003GB002061.

Poorvin, L., J. M. Rinta-Kanto, D. A. Hutchins, and S. W. Wilhelm (2004), Viral lysis as a major source of bioavailable iron in marine ecosystems, *Limnol. Oceanogr.*, *49*, 1734–1741.

Price, N. M., and F. M. M. Morel (1998), Biological cycling of iron in the ocean, in *Metal Ions in Biological Systems*, vol. 35, *Iron Transport and*

Storage in Micro-organisms, Plants and Animals, pp. 1–36, CRC Press, Boca Raton, Fla.

Rich, H. W., and F. M. M. Morel (1990), Availability of well-defined iron colloids to the marine diatom *Thalassiosira weisflogii*, *Limnol. Oceanogr.*, *35*, 652–662.

Roman, M. R., and A. L. Gauzens (1997), Copepod grazing in the equatorial Pacific, *Limnol. Oceanogr.*, *42*, 623–634.

Rueter, J. G., D. A. Hutchins, R. W. Smith, and N. L. Unsworth (1992), Iron nutrition of *Trichodesmium*, in *Marine Pelagic Cyanobacteria: Trichodesmium and Other Diazotrophs*, edited by E. J. Carpenter, D. G. Capone, and J. G. Reuter, pp. 289–306, Springer, New York.

Sedwick, P. N., G. R. DiTullio, D. A. Hutchins, P. W. Boyd, F. B. Griffiths, A. C. Crossley, T. W. Trull, and B. Quéguiner (1999), Limitation of algal growth by iron deficiency in the Australian Subantarctic region, *Geophys. Res. Lett.*, *26*, 2865–2868.

Sieburth, J. M., V. Smetacek, and J. Lenz (1978), Pelagic ecosystem structure: Heterotrophic compartments of the plankton and their relationship to plankton size fractions, *Limnol. Oceanogr.*, *23*, 1256–1263.

Sosik, H. M., and R. J. Olson (2002), Phytoplankton and iron limitation of photosynthetic efficiency in the Southern Ocean during the late summer, *Deep Sea Res., Part I*, *49*, 1195–1216.

Stockner, J. G. (1988), Phototrophic picoplankton: An overview from marine and freshwater ecosystems, *Limnol. Oceanogr.*, *33*, 765–775.

Strom, S. L., C. B. Miller, and B. W. Frost (2000), What sets lower limits to phytoplankton stocks in high-nitrate, low-chlorophyll regions of the open ocean?, *Mar. Ecol. Prog. Ser.*, *193*, 19–31.

Strzepek, R. F., M. T. Maldonado, J. L. Higgins, J. Hall, K. Safi, S. W. Wilhelm, and P. W. Boyd (2005), Spinning the "Ferrous Wheel: The importance of the microbial community in an iron budget during the FeCycle experiment, *Global Biogeochem. Cycles*, *19*, GB4S26, doi:10.1029/2005GB002490, in press.

Tortell, P. D., M. T. Maldonado, and N. M. Price (1996), The role of heterotrophic bacteria in iron-limited ocean ecosystems, *Nature*, *383*, 330–332.

Tortell, P. D., M. T. Maldonado, J. Granger, and N. M. Price (1999), Marine bacteria and biogeochemical cycling of iron in the oceans, *FEMS Microbiol. Ecol.*, *29*, 1–11.

Tovar-Sanchez, A., S. A. Sañudo-Wilhelmy, M. Garcia-Vargas, R. S. Weaver, L. C. Popels, and D. A. Hutchins (2003), A trace metal clean reagent to remove surface-bound iron from marine phytoplankton, *Mar. Chem.*, *82*, 91–99.

Tsuda, A., et al. (2003), A mesoscale iron enrichment in the western subarctic Pacific induces a large centric diatom bloom, *Science*, *300*, 958–961.

Twining, B. S., S. B. Baines, N. S. Fisher, and M. R. Landry (2004), Cellular iron contents of plankton during the Southern Ocean Iron Experiment (SOFeX), *Deep Sea Res., Part I*, *51*, 1827–1850.

Twiss, M. R., and P. G. C. Campbell (1995), Regeneration of trace metals from picoplankton by nanoflagellate grazing, *Limnol. Oceanogr.*, *40*, 1418–1429.

Verity, P. G., C. Y. Robertson, G. R. Tronzo, M. G. Andrews, J. R. Nelson, and M. E. Sieracki (1992), Relationships between cell volume and carbon and nitrogen content of marine photosynthetic nanoplankton, *Limnol. Oceanogr.*, *37*, 1434–1446.

Welschmeyer, N. A. (1994), Fluorometric analysis of chlorophyll *a* in the presence of chlorophyll *b* and pheopigments, *Limnol. Oceanogr.*, *39*, 1985–1992.

Xia, L., A. F. Yakunin, and R. M. L. McKay (2004), Fe-responsive accumulation of redox proteins ferredoxin and flavodoxin in a marine cryptomonad, *Eur. J. Phycol.*, *39*, 73–82.

M. M. D. Al-Rshaidat, R. M. L. McKay, and D. Porta, Department of Biological Sciences, Bowling Green State University, Life Sciences Building, Bowling Green, OH 43403, USA. (mamoona@bgnet.bgsu.edu; rmmckay@bgnet.bgsu.edu; dporta@uwindsor.ca)

P. W. Boyd, National Institute of Water and Atmospheric Research, Centre for Chemical and Physical Oceanography, Department of Chemistry, University of Otago, Dunedin, New Zealand. (pboyd@chemistry.otago.ac.nz)

J. Hall and S. Pickmere, National Institute of Water and Atmospheric Research, Hillcrest, Hamilton, New Zealand. (j.hall@niwa.co.nz; s.pickmere@niwa.cri.nz)

D. A. Hutchins, Graduate College of Marine Studies, University of Delaware, Lewes, DE 19958, USA. (dahutch@udel.edu)

C. E. Mioni and S. W. Wilhelm, Center for Environmental Biotechnology and Department of Microbiology, University of Tennessee, Knoxville, TN 37996, USA. (wilhelm@utk.edu)